Journal of Advanced Chemical Sciences 2(2) (2016) 271–275

ISSN: 2394-5311

Contents List available at JACS Directory

Journal of Advanced Chemical Sciences

journal homepage: www.jacsdirectory.com/jacs

Solid Synthesis and Improved Structural Study of [0.7(Cu_2HgI_4):0.3(AgI_x:$CuI_{(1-x)}$)] of Fast-Ion Conductor (x = 0.2, 0.4, 0.6 and 0.8 Mol. Wt. %)

Noorussaba, Afaq Ahmad*

Department of Chemistry, Solid State Chemistry Lab, Aligarh Muslim University, Aligarh – 202 002, UP, India.

ARTICLE DETAILS

Article history:
Received 30 December 2015
Accepted 29 January 2016
Available online 06 May 2016

Keywords:
Ionic Solids
Fast-Ion Conductor
DTA
DSC
TGA

ABSTRACT

An new series of fast ionic solids in the mixed system [0.7(Cu_2HgI_4):0.3(AgI_x:$CuI_{(1-x)}$)] where x = 0.2, 0.4, 0.6 and 0.8 mol. wt. % respectively by solid state reaction of the appropriate solid mixtures and quenching them at particular temperature. Powdered samples of different compositions containing x mol. wt. % of (AgI_x:$CuI_{(1-x)}$) were synthesized by solid state reactions, using [Cu_2HgI_4] ternary halides as host. Powder specimens of these compositions were analysed using Differential Thermal Analysis (DTA), Differential Scanning Calorimetry (DSC), Thermal Gravimetric Analysis (TGA), Far-Infrared Transmission Spectra (FTIR) and x-ray Powder Diffraction (XRD) techniques. These studies have confirmed the formation of new products as revealed by the absence of diffraction peaks of parent materials in the XRD patterns. Among the various compositions, a significant number of peaks found to contain Ag^+ and Cu^+ in Cu_2HgI_4 respectively and DSC traces have indicated the characteristic β-α phase transition temperature of [0.7(Cu_2HgI_4):0.3(AgI_x:$CuI_{(1-x)}$)] (where x = 0.2, 0.4, 0.6 and 0.8 mol. wt. %) at around 340-545 K. These changes due to crystalline defects or on increased Cu^+-free volume in the tetragonal lattice. In addition, Ag and Cu substitution appears to stabilize the high-temperature, hexagonal structure to temperature well in excess of 340-545 K, associated correspondingly with the melting of the (Ag^+:Cu^+) sublattice and with the storage of iodide/or cadmium and iodide/or mercury sublattices. Fourier transmission infrared spectra of all the fast ionic conductors [0.7(Cu_2HgI_4):0.3(AgI_x:$CuI_{(1-x)}$)] (where x = 0.2, 0.4, 0.6 and 0.8 mol. wt. % respectively) in the wavenumber range extending from 400 to 4000 cm^{-1} are also reported. From these studies the TO and LO models are assigned. FTIR measurements can provide information on the motion and environment of the ions.

1. Introduction

Fast Ion Conductors (FICs) are disordered ionic materials with high electrical conductivity comparable with those of liquid electrolytes and molten salts. Fast ion conductors (i.e. Cu_2HgI_4 etc.) reveal attractive conductivity properties and represents meta-solid state fast ionic conductors [2]. They also arouse interest in their application for chemical sensors [3]. FICs have been interest not only to the technologists as potential materials in solid state ionic devices, but also to the physicists because of their intricate conduction mechanism [4]. The design of electric batteries and potential optical devices requires an understanding of the role of the electronic structure in super ionic conductors [5]. One of the important aspects in understanding super ionic solids is the motion of mobile ions [6]. Several attempts have been made to synthesize new fast ionic solids suitable for electrochemical applications because of their high ionic conductivities at ambient temperatures, while characterization is an essential part in the development of new materials [7]. The new materials are linked by their high ionic conductivities; they display a wide variety of behavior in both the critical region and in the fast ion state [8]. Two routes can lead to improved solid fast ionic conductors, a search for new compounds and structures sustaining high level of ionic conductivity or a modification of existing compounds by heterogeneous or homogeneous doping [9]. Heterogeneous doping, on the contrary, involves mixing with a second phase with very limited solid solubility and for motion of defect concentration profiles in the proximity of interface; the deviation from local electrical neutrality (space charge) is a consequence of point defect equilibrium at interfaces [10]. A number of solids fast ionic conductors undergo a solid phase transition to a high temperature phase accompanied by a sharp jump in ionic conductivity by a factor of ~ 10^4 as well as a structural change [11]. Many fast ionic compounds including those belonging to the A_2BX_4 group (A = Ag and Cu, B = Cd and Hg, X = I) are usually obtained by means of ceramic technology [12-15]. Chemical substitution has been used extensively in recent years to modify either the magnitude of ionic conductivity or the transition temperature separating super ionic and covalent phases in various solid electrolytes [16]. Present work is based on the study of some nominal compositions of [0.7(Cu_2HgI_4):0.3(AgI_x:$CuI_{(1-x)}$)] where x = 0.2, 0.4, 0.6 and 0.8 mol. wt. % respectively using the Differential Thermal Analysis (DTA), Differential Scanning Calorimetry (DSC), Thermal Gravimetric Analysis (TGA), Far-Infrared Transmission Spectra (FTIR) and x-ray Powder Diffraction (XRD) techniques [17]. Copper mercury tetraiodides have long been known to be both fast ion conductors [18, 19] and thermo chromic pigments [20, 21]. Because Cu_2HgI_4 have phase transitions in the 60-70 °C range involving color changes and large changes in ionic conductivity, these thermo chromic materials have also been proposed for various sensors. Recently, the mechanism for the presence or absence of thermochromism in analogues of Cu_2HgI_4 above and below their phase transition temperature has been reported [21]. The temperature dependent thermochromism is due to changes in the charge transfer spectra arising from the donation of electron charge from the filled p-orbitals of the iodide ligands to the unfilled d-orbitals of the mercury atom. The phase transition is considered to be an order-disorder type. The low temperature, β-phase for Cu_2HgI_4 are both tetragonal but they differ in the placement of the A^+ cations and vacancy. In the high temperature, α- phase, the iodide sublattice is retained while cations are distributed randomly among all sites. Thus, they (A_2BX_4) are isostructural in their α- phases, clearly, them, the A^+ cations plays a role in the exact structure in the low temperature form and determines, for the most part, the conductivity, phase transition temperature and thermo chromic properties [22].

In such ternary superionic conductors mobile ions of different type contribute to the total electric conductivity and thus result in different vibration frequencies. In their turn, the vibration frequencies reflect the

*Corresponding Author
Email Address: afaqahmad21@gmail.com (Afaq Ahmad)

Cite this Article as: Noorussaba, Afaq Ahmad, Solid synthesis and improved structural study of [0.7(Cu_2HgI_4):0.3(AgI_x:$CuI_{(1-x)}$)] of fast-ion conductor (x = 0.2, 0.4, 0.6 and 0.8 mol. wt. %), J. Adv. Chem. Sci. 2(2) (2016) 271–275.

interaction between the lattice and charge carriers. From this point of view IR spectroscopy provides an effective understanding of resonant processes in solid electrolytes as it is very sensitive to temperature induced phase transitions affecting nearest neighbor dynamics. Although the lattice dynamics of Ag_2MX_4 family representatives was extensively studied [22].

2. Experimental Methods

2.1 Materials

The following materials were used as received mercury [II] iodide, silver iodide and cuprous iodide were of CDH anal grade (India) and SD fine-chem. India, each of which had a purity of 99%, 99% and 99% respectively.

2.2 Preparation of Pure and Doped Samples of [0.7(Cu_2HgI_4):0.3(AgI_x:$CuI_{(1-x)}$)]

2.2.1 Preparation of Pure Sample [Cu_2HgI_4]

Cu_2HgI_4 was prepared by reaction of a stoichiometric mixture of the component binary halides CuI and HgI_2 according to the equation:

$$2CuI + HgI_2 \rightarrow Cu_2HgI_4 \quad (4)$$

The powdered raw materials were mixed, the fine ground stoichiometric mixture of the binary components was sealed in an ampoule and was placed in an air oven (CE 0434 NSW-144) at approximately 200 °C for 24 h and finally cooled rapidly to room temperature (removal from furnace at 200 °C). After cooling, the dark red color changed to maroon. Cu_2HgI_4 is dark red below 76 °C and maroon after 76 °C [23].

2.2.2 Preparation of Doped Sample [0.7(Cu_2HgI_4):0.3(AgI_x:$CuI_{(1-x)}$)]

AgI and CuI were mixing in various x = 0.2, 0.4, 0.6 and 0.8 mol. wt. % respectively in an Agate motar to form A_2BX_4 mixture by solid state reaction. Now copper tetraiomercurate 0.7 mol. wt. % [Cu_2HgI_4] were doped by 0.3 mol. wt. % (AgI_x:$CuI_{(1-x)}$) composite mixture to form [0.7(Cu_2HgI_4):0.3(AgI_x:$CuI_{(1-x)}$)] fast ion conductor, in an Agate mortar at room temperature and heating then at 200 °C (473 K) for 24 hrs in a silica crucible. After intermittent grinding, all the samples were prepared [24].

2.3 Characterization of Pure and Doped Samples of [0.7(Cu_2HgI_4): 0.3(AgI_x:$CuI_{(1-x)}$)]

2.3.1 X-Ray Powder Diffraction Studies

X-ray powder diffraction were performed for all the fast ionic composite systems [0.7(Cu_2HgI_4):0.3(AgI_x:$CuI_{(1-x)}$)] x = 0.2, 0.4, 0.6 and 0.8 mol. wt. % respectively after the reaction was completed using Rigaku Rad B powder diffractometer and a Bruker AXS D8 Advance diffractometer with a K-beta filter with Cu-Kα (λ = 1.54060 Å) radiation at room temperature. The angle range for measurement was from 10 °C to 70 °C and the scanning speed was 1° min^{-1}. The X-ray diffractogram values of all the composite samples [0.7(Cu_2HgI_4):0.3(AgI_x:$CuI_{(1-x)}$)] correspond to standard values of [Cu_2HgI_4] and careful analysis revealed that in addition to standard peaks of pure host [Cu_2HgI_4], a number of peaks appeared for the (AgI_x:$CuI_{(1-x)}$)-doped host composite system.

2.3.2 FTIR Measurements

The IR spectrum was recorder for all the fast ionic composite systems [0.7(Cu_2HgI_4):0.3(AgI_x:$CuI_{(1-x)}$)] (where x = 0.2, 0.4, 0.6 and 0.8 mol. wt. % respectively) in the mid-infrared range 400-4000 cm^{-1} (25-25 μm) at room temperature using a INTERSPEC-2020, FTIR spectrophotometer measured in KBr.

2.3.3 Thermal Analysis

Differential Thermal Analysis (DTA), Differential Scanning Calorimetry (DSC) and Thermo-Gravimetric Analysis (TGA) was carried out on [0.7(Cu_2HgI_4):0.3(AgI_x:$CuI_{(1-x)}$)] mixed composite samples, using DTG-60H thermal analyser in nitrogen atmosphere with flow rate of 30 mL min^{-1} and heating rate 25 °C min^{-1} in the temperature range 20-500 °C. The reference used was 10 mg alumina powder.

3. Result and Discussion

3.1 FTIR Analysis

3.1.1 FTIR Discussion in Cu_2HgI_4

As in Ketelaar description, the α-phase retains the same iodine structure as in the β phase. While the cation and vacancy sites becomes equivalent [1]. Later studies [2, 3] showed that the low temperature phases are tetragonal and in addition, are not isostructural, differing in the placement of the two monovalent cation (Ag or Cu) and vacancy. Thus based on data from the best single crystals, i.e. tetragonal β-phase was the only stable low-temperature phase and the apparent phase change after cycling could be explained by the formation of domains with the tetragonal c axis randomly oriented along the three spatial axes, thus giving the impression of a cubic lattice. The interpretation of a single low-temperature phase has the broadest base of support of the two views at present [3]. Assuming the β phase is tetragonal, the number and symmetry of normal modes can be determined. Group theory analysis finds the following number and symmetries for the 18 optical modes in each materials.

Cu_2HgI_4: $2A_1 + A_2 + 2B_1 + 3B_2 + 5E$

The Infrared and Raman selection rules give the following allowed mode symmetries.

Infrared	Raman
Cu2HgI4:$3B_2 + 5E$	$2A_1+A_2+2B_1 + 3B_2 + 5E$
(8 Bands)	(12 Bands)

Using projection operators, we find that the B symmetry mode involve motion of the cation along the tetragonal c axis (z), and the E modes involve motion of the cations, along the a and b axes (x or y), B mode couple to electric fields along the z axis and E modes couple to fields in the xy plane, so that FTIR spectra would determine the mode-symmetry assignments uniquely [4-7].

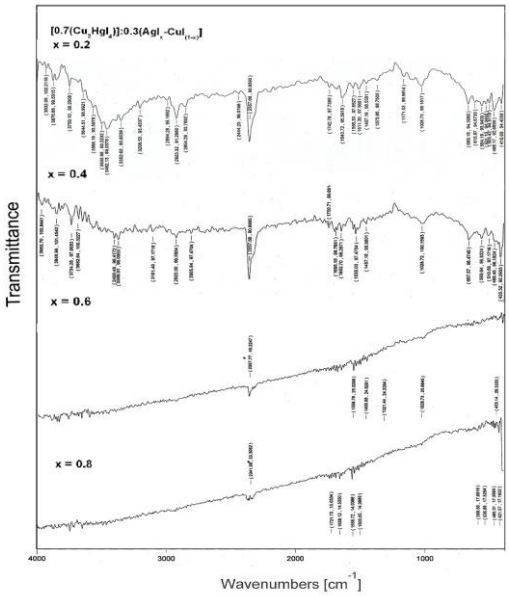

Fig. 1 FTIR spectrum for [0.7(Cu_2HgI_4):0.3(AgI_x:$CuI_{(1-x)}$)] fast ionic conductors (where x = 0.2, 0.4, 0.6 and 0.8 mol. wt. %)

Table 1 The irreducible representation for the 15 predicted modes of β-Cu_2HgI_4

Modes	Cu_2HgI_4
Internal modes (HgI_4)	
stretch	A_1+B_2+E
Deformation	$A_1+B_1+B_2+E$
External modes (HgI_4)	
rotatory	A_2+E
translational	B_2+E
External Modes (Cu or Ag)	
translational	B_2+E
Acoustic Modes	B_2+E

3.1.2 Factor Group Analysis Cu_2HgI_4

The Wigner-Seitz cell for β-Cu_2HgI_4 shown in Fig. 1 belongs to the D_{2d} point group. The irreducible representation for the 15 IR allowed modes are listed in Table 1 [6], with the D_{2d} - S_4 correlation being A_1 and A_2 to A, B_1 and B_2 to B and E to E. Fig. 1 shows FTIR spectrum for [0.7(Cu_2HgI_4):0.3(AgI_x:$CuI_{(1-x)}$)] fast ionic conductors where x = 0.2, 0.4, 0.6 and 0.8 mol. wt. %. In the IR spectra of [0.7(Cu_2HgI_4):0.3($AgI_{0.8}$:$CuI_{0.2}$)] the 2341 cm^{-1} peak in Table 2 is strongest in xx, yy and zz direction making it an A1. The A1 peak shifted in x = 0.4, 0.6 and 0.8 at 2357.77, 2357.66, 2357.66 cm^{-1}. The peak at 1558.72 cm^{-1} and 1503.05 cm^{-1} are strongest in the xx and yy polarizations and therefore belongs to A1 or B1 classes. This peak shifted in x = 0.4, 0.6 and 0.8 mol. wt. % composites are 1558.76,

1459.88 cm^{-1} for x = 0.4, 1643.72, 1511.30 cm^{-1} for x = 0.6 and 1695.18, 1535.03 cm^{-1} for x = 0.8 mol. wt. %. The only noticeable peaks in xz polarization and E symmetry is at 421.57 cm^{-1} and the 1000 cm^{-1} shoulder appears to be weak in xx, zz and xz polarization making it likely that at least some of the peaks causing this feature would be maximized in the xy polarization and therefore of B_1 symmetry in x = 0.2 mol. wt. % are at 459. E_1 symmetry peaks are found in x = 0.4, 0.6 and 0.8 are at 459.14 cm^{-1}, 468.17 cm^{-1} and 667.57 cm^{-1}. The shoulder peaks appears in x = 0.4, 0.6 and 0.8 are 1028.73, 1028.73 and 1028.72 cm^{-1} respectively. This leaves three weak peaks at 588.56, 536.88 and 463.31 cm^{-1} in x = 0.2 which shifted in x = 0.6 and 0.8 are at 615.87, 564.18, 531.10 cm^{-1} and 569.64, 510.56 and 469.45 cm^{-1} respectively whereas in x = 0.4, these weak peaks are absent.

Table 2 [0.7(Cu_2HgI_4):0.3(AgI_x:$CuI_{(1-x)}$)] fast ionic conductors (where x = 0.2, 0.4, 0.6 and 0.8 mol. wt. %) room temperature peaks and assignments

[0.7(Cu_2HgI_4): 0.3$(AgI)_{(0.8)}$: $CuI_{(0.2)}$)]		[0.7(Cu_2HgI_4): 0.3$(AgI)_{(0.6)}$: $CuI_{(0.4)}$)]		[0.7(Cu_2HgI_4): 0.3$(AgI)_{(0.4)}$: $CuI_{(0.6)}$)]		[0.7(Cu_2HgI_4): 0.3 $(AgI)_{(0.2)}$: $CuI_{(0.8)}$)]	
Peaks (cm^{-1})	Assign ments	Peaks (cm^{-1})	Assign ments	Peaks (cm^{-1})	Assign ments	Peaks (cm^{-1})	Assign ments
2341	A_1	2357.77	A_1	2357.66	A_1	2357.66	A1
1558	A_1	1558.76	A_1		A_1	1695.18	A1
1000	-	1028.73	-	1643.72	-	1028.72	-
1503	B_1	1459.88	B_1	1028.73	B_1	1535.03	B1
421	B_2	459.14	B_2	1511.30 468.17	B_2	667.57	B2

Unassigned and a speculatively assignment for the 1000 cm^{-1} feature. The band seen at 588.50 cm^{-1} arises from HgI_2 contamination. Also the 536.88 cm^{-1} peak may be spurious because it is not observed at low temperature or in room temperature spectra of polycrystalline samples. HgI_2 contamination peaks also seen in x = 0.6 and 0.8 mol. wt. % at 669.18, 615.87cm^{-1} and 667.57, 569.64 cm^{-1} respectively. Peaks of B_2 and E symmetry are allowed in the IR spectra and should be strong peaks, the occurrence of 420.57 cm^{-1} (x = 0.2) peak in the IR strengthens the E assignment for the peak at 421.57 cm^{-1}. For the x = 0.4, 0.6 and 0.8 mol. wt. % the peaks are at 458.14, 409.90 and 419.32 cm^{-1} respectively.

3.1.3 FTIR Comparison in Cu_2HgI_4

The IR active peaks with symmetry assignments are listed in Table 3. For [0.7(Cu_2HgI_4):0.3($AgI_{0.x}$:$CuI_{(1-x)}$)] in Table 3, 2341.99, 2357.77, 357.66, 2357.66 cm^{-1} A1 peak is assigned as the HgI_4^{-2} symmetric stretch [6]. Pressure dependence peak at 1558, 1558.76, 1643.72 and 1695 cm^{-1} resembles that of a symmetry feature respectively [8]. This correlation implies that the 1558 cm^{-1}, peaks in [0.7(Cu_2HgI_4):0.3($AgI_{0.x}$:$CuI_{(1-x)}$)] has 1558.76, 1643.72 and 1695 cm^{-1} A_1 symmetry. The peak at 588.56, 669.18, 667.57 cm^{-1} in x = 0.2, 0.6 and 0.8 mol. wt. % of Cu_2HgI_4 can be assigned as B_1 symmetry. Factor group analysis for β-Cu_2HgI_4 shows only two A_1 modes, the HgI_4^{2-} symmetric stretch and a mode which may be described as HgI_4^{2-} symmetric deformation assigned to the (1558, 1558.76, 1643.72 and 1695 cm^{-1}) in Cu_2HgI_4 composites respectively. This HgI_4^{2-} deformation may be described as a stretch of Cu-I and Ag-I bonds. The broadening of the (1558, 1558.76, 1643.72 and 1695 cm^{-1}) peaks in β-Cu_2HgI_4, as the temperature is increased toward the temperature of the phase transition also suggests that these modes are associated with Cu-I and Ag-I motion respectively.

Table 3 [0.7(Cu_2HgI_4):0.3(AgI_x:$CuI_{(1-x)}$)] fast ion conductors, where (x = 0.2, 0.4, 0.6 and 0.8 mol. wt. %), room temperature peaks and assignment

Far-IR transmission peaks (cm^{-1})					
[0.7(Cu_2HgI_4): 0.3$(AgI)_{(0.8)}$: $CuI_{(0.2)}$)]	[0.7(Cu_2HgI_4): 0.3$(AgI)_{(0.6)}$: $CuI_{(0.4)}$)]	[0.7(Cu_2HgI_4): 0.3$(AgI)_{(0.4)}$: $CuI_{(0.6)}$)]	[0.7(Cu_2HgI_4): 0.3$(AgI)_{(0.2)}$: $CuI_{(0.8)}$)]	Sym-metry	Assignment
2341.99	2357.77	2357.66	2357.66	A1	HgI_4^{2-} Symmetric stretch
1558	1558.76	1643.72	1695	A1	HgI_4^{2-}de-formation, M-I stretching
1000	1028.73	1028.73	1028.73	-	De-formation
1503	1459.88	1511.30	1535.03	B1	Cu-I, Ag-I symmetric stretch
421.57	459.14	468.17	420.32	E	Cu+, Ag +attempt frequency

This behavior contrasts with that of the (2341.99, 2357.77, 357.66, 2357.66 cm^{-1}) peaks in β-Cu_2HgI_4 respectively, which remain sharp up to the order-disorder phase transitions. The pressure dependence also is consistent with an assignment in which (1558, 1558.76, 1643.72 and 1695 cm^{-1}) peaks involve copper iodide motion [5]. In β-Cu_2HgI_4, the Cu-I stretch is contained in a linear modes E (xy_{trans})–E (xy_{rot}) [9] and possibly one or both of the two weak peaks seen between 3780 and 420.57 cm^{-1} at low temperature can be assigned as the Cu-I or Ag-I symmetric stretch (at room temperature). The pressure the low frequency modes in β-Cu_2HgI_4 is expected to have several Hg-I and Cu-I deformation with the Hg-I deformations at higher frequency than those of Cu-I. The low frequency E modes at (432.66, 424.72, 431.65 and 431.45 cm^{-1}) in β-Cu_2HgI_4, are of special interest.

Thus this indicates that these modes involve large components of Cu and Ag motions. Accordingly, these E symmetry features are assigned as external Cu^+ or Ag^+ translational modes in the xy plane. The E and B_2 symmetry coordinates for Cu^+ translation, the former symmetry coordinates corresponds to Cu translation in the xy plane and the latter to Cu translation along the z axis.

A linear combination of the E and B_2 symmetry coordinates may be formed in which cation motion occurs in the direction of the tetrahedral face of four iodide ions. The probable Cu^+ and Ag^+ conduction path involves Cu^+ and Ag^+ motion through this face, into an octahedral site, and through another I_3 triangular face into a tetrahedral site [7]. The values assigned to the attempt frequencies in Cu_2HgI_4 are similar to cation translational modes in related electrolytes [7].

Inspection of Table 2 and Fig. 1, shows that IR spectra of all [0.7(Cu_2HgI_4):0.3(AgI_x:$CuI:_{(1-x)}$)], conductors exhibit the strongest feature at 1539.77 cm^{-1}, 1643.72, 1535.03, 1558.76 and 1558.72 cm^{-1} respectively, while the infrared activity below 900 cm^{-1} is weak. On the basis of the above discussion, these results strongly suggest that the existence of $(HgI_4)_2^{2-}$/(Ag^+:Cu^+) tetrahedral in the x = 0.2 and 0.8 mol. wt. % (Ag^+:Cu^+)-doped fast ionic conductors should be excluded at least in concentration detectable by infrared spectroscopy.

Therefore, it is found that the infrared activity of the x = 0.2 and x = 0.8 mol. wt. % (Ag^+:Cu^+)-fast ionic conductors arises from $(HgI_4)_2^{2-}$ while x = 0.4 mol. wt. % (Ag^+:Cu^+)-fast ionic conductors show weakest feature at lower frequencies. Increasing the Ag^+:Cu^+ content induces a decreases to increase of the infrared activity in [0.7(Cu_2HgI_4):0.3(AgI_x:$CuI:_{(1-x)}$)] [11].

3.2 X-Ray Diffraction

Fig. 2 shows the typical XRD diffractogram obtained for four different ternary halides doped with different compositions of [0.7(Cu_2HgI_4):0.3(AgI_x:$CuI_{(1-x)}$)] composites (x = 0.2, 0.4, 0.6 and 0.8 mol. wt. %) respectively. In γ-AgI, iodide ions are known to form a mixture of close packed structures, at temperatures well below 420 K (140 °C) consisting of fcc and hcp structures which are commonly designated as γ-AgI and β-AgI respectively. However, for pedagogical reasons only γ-AgI is considered at room temperature. According, to the xrd data obtained during the present study have been compared with that of γ-AgI. It is clear from Table 4 that all the xrd data contain 2θ values different from that of the starting materials. Also it is obvious from Table 5, that the above compositions are polycrystalline in nature consisting of a multiphase mixture of AgI and / CuI phases. These phases have been identifies as follows.

(a) [0.7(Cu_2HgI_4):0.3($AgI_{0.8}$:$CuI_{0.2}$)]-doped composites.
In case of [0.7(Cu_2HgI_4):0.3($AgI_{0.8}$:$CuI_{0.2}$)]-doped composites system, the peaks at 22.38°, 29.15°, 41.88° and 59.26° can be attributed to the presence of γ-AgI, whereas peaks observed at 26.40° and 55.86° have been compared with that of $CuICu_2HgI_4$. In addition, γ-CuI lines have also been observed at 16.41°, 20.03° and 33.615°. $AgICu_2HgI_4$ lines are at 39.76° is also found. Pure Cu_2HgI_4 lines 25.56°, 45.28°, 60.76°, 63.51° and 67.13° respectively. Effectively the composition of [0.7(Cu_2HgI_4):0.3($AgI_{0.8}$:$CuI_{0.2}$)]-doped composites system consists of γ-AgI, $CuICu_2HgI_4$, γ-CuI, $AgICu_2HgI_4$, and pure Cu_2HgI_4 phases (Table 4) [25].

(b) [0.7(Cu_2HgI_4):0.3($AgI_{0.6}$:$CuI_{0.4}$)]-doped composites.
In case of [0.7(A_2BX_4):0.3($AgI_{0.6}$:$CuI_{0.4}$)]-doped composites system, the peaks observed at 23.22° alone could be attributed to the presence of γ-AgI in Cu_2HgI_4. Another interesting feature of this particular compositions is that the xrd pattern is quite broad in shape thus suggesting its highly disordered nature. However, small traces of silver aggregates may be present in this composite material. Since very faint lines observed at 29.15°, 45.06° could only be attributed to the presence of small traces of metallic silver in Cu_2HgI_4, respectively (Table 4) [25].

(c) $[0.7(Cu_2HgI_4):0.3(AgI_{0.4}:CuI_{0.6})]$-doped composites.
The xrd data corresponding to the composition having $(AgI_{0.4}:CuI_{0.6})]$-doped composites of Cu_2HgI_4 system appears to suggest that γ-CuI may be the major content in the dopant materials because of the fact that lines observed at 2θ = 16.23°, 19.60° and 33.61° could be fittingly attributed to the presence of γ-CuI. However, peaks observed at 2θ = 26.40° and 51.83° can be attributed to the presence of $CuICu_2HgI_4$ as a constituent in the multiphase system (Table 4) [25].

(d) $[0.7(Cu_2HgI_4):0.3(AgI_{0.2}:CuI_{0.8})]$-doped composites
In case of the sample having $[0.7(Cu_2HgI_4):0.3(AgI_{0.2}:CuI_{0.8})]$-doped composites system, the observed xrd peaks at 16.19° and 33.61° may be attributed to the formation of CuI while the peak at 66.91° could be attributed to the presence of $CuICu_2HgI_4$. Remaining unidentified peaks may be due to the presence of certain silver based compounds. From the above xrd analysis it is clear that all composite fast ionic conductors have been formed during the present investigation (Table 4) [25].

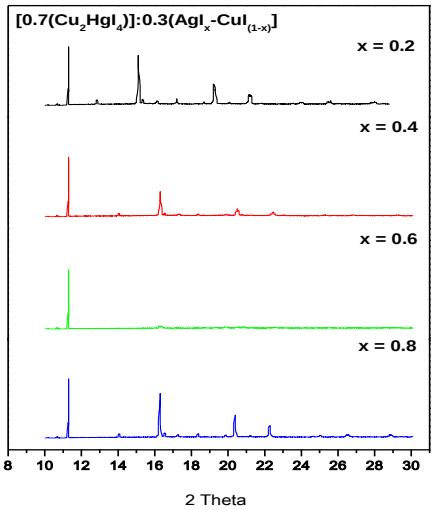

Fig. 2 X-ray diffractogram for $[0.7(Cu_2HgI_4):0.3(AgI_x:CuI_{(1-x)})]$ fast ionic conductors (where x = 0.2, 0.4, 0.6 and 0.8 mol. wt. %)

Table 4 X-ray diffractogram peaks and assignment for $[0.7(Cu_2HgI_4):0.3(AgI_x:CuI_{(1-x)})]$ fast ion conductors

$[0.7(Cu_2HgI_4):0.3(AgI)_{(0.8)}:CuI_{(0.2)})]$		$[0.7(Cu_2HgI_4):0.3(AgI)_{(0.6)}:CuI_{(0.4)})]$		$[0.7(Cu_2HgI_4):0.3(AgI)_{(0.4)}:CuI_{(0.6)})]$		$[0.7(Cu_2HgI_4):0.3(AgI)_{(0.2)}:CuI_{(0.8)})]$	
2θ	Peak Assignment	2θ	Peak Assignment	2θ	Peak Assignment	2θ	Peak Assignment
16.41,	CuI	23.22	γ-AgI	16.23	γ- CuI	16.19	γ- CuI
20.03	AgI			19.60	γ- CuI	33.61	γ- CuI
21.38	Cu_2HgI_4	29.15	Metallic silver	33.61	γ- CuI		
25.56	$CuICu_2HgI_4$	45.06	metallic silver	26.40 51.83	$CuICu_2HgI_4$ $CuICu_2HgI_4$	66.91	CuICu2HgI4
26.40	AgI						
29.15	CuI						
33.61	$AgICu_2HgI_4$						
39.76	AgI						
41.88	Cu_2HgI_4						
45.38	$CuICu_2HgI_4$						
55.86	AgI						
59.26							
60.76	Cu_2HgI_4						
63.13	Cu_2HgI_4						
67.13	Cu_2HgI_4						

Table 5 DSC endothermic peaks for $[0.7(Cu_2HgI_4):0.3(AgI_x:CuI_{(1-x)})]$ fast ionic conductors (where x = 0.2,0.4, 0.6 and 0.8 mol. wt. %)

Composition	Endothermic Peaks (K)		
	I	II	III
$[0.7(Cu_2HgI_4):0.3(AgI)_{(0.2)}:CuI_{(0.8)})]$	343	423	563.97
$0.7(Cu_2HgI_4):0.3(AgI)_{(0.4)}:CuI_{(0.6)})$	378	453	588.16
$[0.7(Cu_2HgI_4):0.3(AgI)_{(0.6)}:CuI_{(0.4)})]$	356.53	464.31	633
$[0.7(Cu_2HgI_4):0.3(AgI)_{(0.8)}:CuI_{(0.2)})]$	359.5	464	340

3.3 Thermal Analysis

3.3.1 Differential Scanning Calorimetry (DSC)

Fig. 3 depicts the DSC thermograms recorded for the four different samples in the mixed fast ionic composite systems $[0.7(Cu_2HgI_4):0.3(AgI_x:CuI_{(1-x)})]$ (x = 0.2, 0.4, 0.6 and 0.8 mol. wt. %).

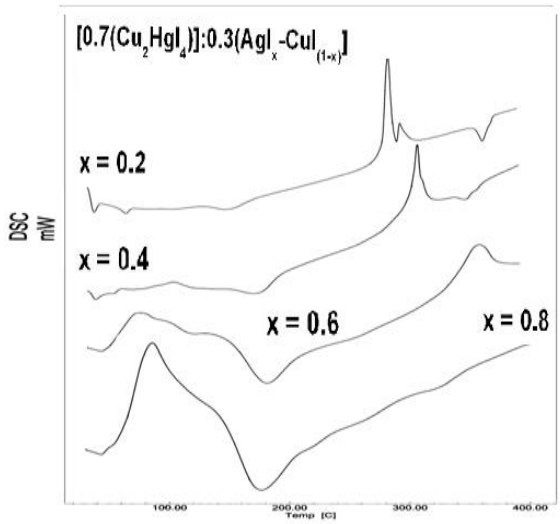

Fig. 3 DSC for $[0.7(Cu_2HgI_4):0.3(AgI_x:CuI_{(1-x)})]$ fast ionic conductors (where x = 0.2, 0.4, 0.6 and 0.8 mol. wt. %)

It is clear from Fig. 3 and Table 5, DSC traces recorded for various compositions of $[0.7(Cu_2HgI_4):0.3(AgI_x:CuI_{(1-x)})]$ were found to exhibit certain interesting feature. For instance, DSC curves obtained for the compositions containing x = 0.2, 0.4 and 0.6 mol. wt. % of Cu_2HgI_4 exhibited endothermic peaks at 563.97 K, 588.16 K and 633 K respectively for the attributed to the γ-β phase transition temperature of the CuI-AgI solid solutions present within these specimens, whereas those for the remaining composition x = 0.8 mol. wt. % was found to be featureless as shown in fig 4. On the other hand the exothermic peaks obtained in dsc curves of all the composites are at 423 K, 453 K, 463.31 K and 463 K respectively. Clearly, the above mentioned exothermic peaks are comparable to that of β-α phase transition of pure AgI (≈ 420 K). The DSC results therefore suggest that the combination of the two starting materials namely (AgI:CuI) and Cu_2HgI_4 is complete for a composition around 50 mol. % Cu_2HgI_4 resulting in the formation of new substances which are probably Ag+ ion conductors having very small traces of AgI [26].

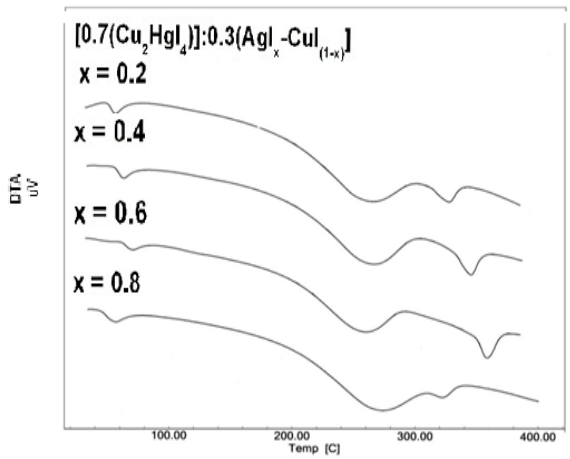

Fig. 4 DTA for $[0.7(Cu_2HgI_4):0.3(AgI_x:CuI_{(1-x)})]$ fast ionic conductors (where x = 0.2, 0.4, 0.6 and 0.8 mol. wt. %)

3.3.2 Differantial Thermal Analysis (DTA)

DTA curves for all the sixteen samples composition $[0.7(Cu_2HgI_4):0.3(AgI_x:CuI_{(1-x)})]$, are shown in Fig. 4. On comparing these curves, we note the following important features.

(1) A well-defined intense peak prepared at ~ 353-393 K in all curves. This peak corresponds to a β-α- like transition of the host $[Cu_2HgI_4]$. The peak strength has increased on further doping of x mol. wt. % of

(AgI:CuI). This is indicative of partial and complete stabilization of the high conducting α- like phase of the host [58] in the samples respectively. These observations are exactly correlate our DSC results [27].

(2) A second intense and well defined peak appeared at ~ 513-553 K in all the DTA curves of Cu_2HgI_4 system. This peak obviously corresponds to the β – α like transition of CuI-AgI solid solutions. This β – α phase transition peak becomes broad with (AgI_x:$CuI_{(1-x)}$) content, this is due to the form of crystalline phase within space charge layer that is expected to form between (AgI:CuI) and [Cu_2HgI_4 [28].

(3) It has been observed from the DTA curves of [0.7(Cu_2HgI_4):0.3(AgI_x:$CuI_{(1-x)}$)], that an additional peak is obtained after the β – α phase transition peak with the addition of (AgI_x:$CuI_{(1-x)}$) and its intensity increase with the mole fraction of (AgI:CuI). This peak attributed to interface interactions between (AgI_x:$CuI_{(1-x)}$) and [Cu_2HgI_4]. The above results clearly reveal the partial presence of fast ionic phase in all the samples.

3.3.3 Thermo-Gravimetric Analysis (TGA)

TGA curves for (AgI_x:$CuI_{(1-x)}$)-doped host samples, it shifts to a lower temperature because of the interaction between dopant (AgI_x:$CuI_{(1-x)}$) and host [Cu_2HgI] (where x = 0.2, 0.4, 0.6 and 0.8 mol. wt. %). In the TGA curves of [0.7(Cu_2HgI_4):0.3(AgI_x:$CuI_{(1-x)}$)] [Fig. 5], from room temperature up to about 400 °C. One distinct peak of TGA are obtained for the [0.7(Cu_2HgI_4):0.3(AgI_x:$CuI_{(1-x)}$)], in the temperature range 400–500 °C with corresponding mass loss for pure samples, and for (AgI_x:$CuI_{(1-x)}$)-doped host samples [29] are shown. These data corroborate the observations of TGA studies.

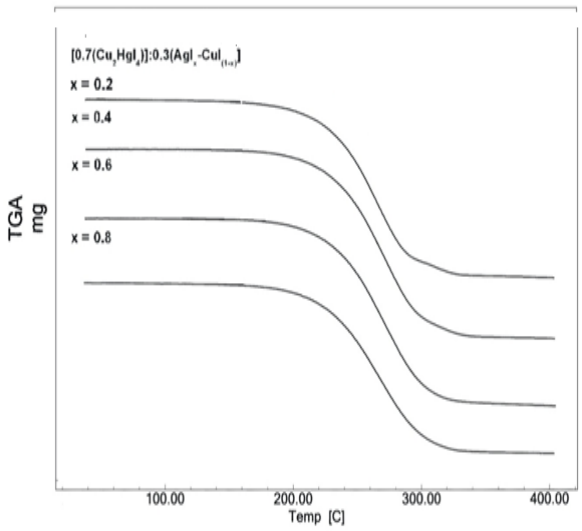

Fig. 5 TGA for [0.7(Cu_2HgI_4):0.3(AgI_x:$CuI_{(1-x)}$)] fast ionic conductors (where x = 0.2, 0.4, 0.6 and 0.8 mol. wt. %)

4. Conclusion

Thus, novel composite fast ion conductors [0.7(Cu_2HgI_4):0.3(AgI_x:$CuI_{(1-x)}$)], were prepared and investigated by X-ray powder diffraction, FTIR spectral analysis, Differential Thermal Analysis (DTA), Differential Scanning Calorimetry (DSC) and Thermo Gravimetric Analysis (TGA) studies to confirmed the formation of all the fast ion conductors. Whereas [0.7(Cu_2HgI_4):0.3(AgI_x:$CuI_{(1-x)}$)] composite fast ion conductors were prepared and investigated also by X-ray powder diffraction, FTIR spectral analysis, Differential Thermal Analysis (DTA), Differential Scanning Calorimetry (DSC) and Thermo Gravimetric Analysis (TGA) studies to confirmed the formation of all the fast ion conductors.

Acknowledgement

The authors are gratefully acknowledged to UGC New Delhi for financial assistance as UGC-PDF Women Scientist Scheme. The authors also gratefully acknowledge the Chairman of the Department of Chemistry for providing the research facilities.

References

[1] H.W. Zandbergen, The crystal structure of α-thallium hexaiodochromate, α-Tl_4CrI_6, Acta Cryst. B 35 (1979) 2852-2855.
[2] A.V. Franiv, O.S. Kushnir, I.S. Girnyk, V.A. Franiv, I. Kityk, M. Piasecki et al, Growth and optical anisotropy of Tl_4CdI_6 single crystals, Ukr. J. Opt. 14 (2013) 6-13.
[3] D.S. Kalyagin, Y.E. Ermolenko, Y.G. Vlasov, Diffusion of Tl-204 isotope and ionic conductivity in Tl_4HgI_6 membrane material for chemical sensors, Rus. J. Appld. Chem. 81 (2008) 2172-2174.
[4] M. Hassan, M.S. Nawaz, Rafiuddin, Ionic conduction and effect of immobile cation substitution in binary system (AgI)4/5-(PbI_2)1/5, Radiat. Eff. Defects Solids 163 (2008) 885-891.
[5] K. Wakamura, Characteristic properties of dielectric and electronic structures in super ionic conductors, Solid State Ionics 149 (2002) 73-80.
[6] R. Sudharsanan, T.K.K. Srinivasan, Radhakrishna, Raman and far IR studies on Ag_2CdI_4 and Cu_2CdI_4 superionic compounds, Solid State Ionics, 13 (1984) 277-283.
[7] A. Viswanathan, S. Austin Suthanthiraraj, Impedance and modulus spectroscopic studies on the fast ion conducting system CuI-Ag_2MoO_4, Solid State Ionics 62(1–2) (1993) 79-83.
[8] H.G. Le Duc, L.B. Coleman, Far-infrared studies of the phase transition and conduction mechanism in the fast-ion conductors Ag_2HgI_4 and Cu_2HgI_4, Phys. Rev. B 31 (1985) 933-941.
[9] P. Knauth, Ionic conductor composites: theory and materials, J. Electroceram. 5 (2000) 111-125.
[10] J. Mair, Ionic conduction in space charge regions, Prog. Solid State Chem., Bull. Mater. Sci. 23 (1995) 171-263.
[11] E.A. Secco, A. Sharma, Structure stabilization: locking-in fast cation conductivity phase in Tl I, J. Phys. Chem. Sol. 2 (1995) 251-54.
[12] J.B. Goodenough, Ceramic solid electrolytes, Solid State Ionics 94 (1997) 17-25.
[13] S. Geller, Solid Electrolytes, Springer, Berlin, 1977.
[14] S. Hull, Superionics: crystal structures and conduction processes, Rep. Prog. Phys. 67 (2004) 1233-1314.
[15] R.C. Agrawal, R.K. Gupta, Superionic solid: composite electrolyte phase-an overview, J. Mater. Sci. 6(34) (1995) 1131-1162.
[16] R.B. Beeken, J.C. Faludi, W.M. Schreier, J.M. Tritz, Ionic conductivity in Cu-substituted Ag_2CdI_4, Solid State Ionics 154-155 (2002) 719-722.
[17] Noorussaba, I.M. Khan, A. Ahmad, Synthesis and structural transformation of [0.7(Ag_2CdI_4):0.3(AgI_x:$CuI_{(1-x)}$] of fast ion conductor (where x = 0.2, 0.4, 0.6 and 0.8 mol. wt. %), J. Adv. Electrochem. 2(1) (2016) 32-36.
[18] S. Shao-rui, X. Ding-guo, An ab-initio calculation study on the super ionic conductors α-AgI and Ag_2X (X = S, Se) with BCC structure, Solid State Ionics 179 (2008) 2330-2334.
[19] H. Liu, L. Tan, Synthesis, structure and electrochemical properties of $CdMoO_4$ nanorods, Ionics 16 (2010) 57-60.
[20] K. Funke, AgI-type solid electrolytes, Prog. Solid State Chem. 11 (1976) 345-402.
[21] H.R.C. Jaw, M.A. Mooney, T. Novinson, W.C. Kaska, J.I. Zink, Optical properties of the thermochromic compounds disilver tetraiodomercurate(2-) and dicopper tetraiodomercurate(2-), Inorg. Chem. 26 (1987) 1387-1391.
[22] E. Kartini, T. Sakuma, K. Basar, M. Ihsan, Mixed cation effect on silver-lithium solid electrolyte $(AgI)_{0.5}(LiPO_3)_{0.5}$, Solid State Ionics 179 (2008) 706-711.
[23] E.A. Secco, M.G. Usha, Cation conductivity in mixed sulfate-based compositions of Na_2SO_4, Ag_2SO_4, and Li_2SO_4, Solid State Ionics 68 (1994) 213-219.
[24] Noorussaba, Afaq Ahmad, Phase transition in a [Ag_2HgI_4:0.2AgI] mixed composite systems doped with KI, Russ. J. Electrochem. 49 (2013) 1065-1072.
[25] V. Fernandez, F. Jaque, J.M. Calleja, Raman and optical absorption spectroscopic study of the thermochromic phase transition of Ag_2HgI_4, Solid State Commun. 59 (1986) 803-807.
[26] P. Varshney, Sarita, A. Ahmad, S. Beg, Study of phase transition in ZrO_2 doped with Pb_3O_4, J. Phys. Chem. Solids 67 (2006) 2305-2309.
[27] R.C. Agrawal, R. Kumar, A. Chandra, Transport studies on a new fast silver ion conducting system :0.7[0.75AgI:0.25AgCl]:0.3 [yAg_2O:(1− y)B_2O_3], Solid State Ionics 84 (1996) 51-60.
[28] S. Sultana, R. Rafiuddin, Enhancement of ionic conductivity in the composite solid electrolyte system: TlI–Al_2O_3, Ionics 15 (2009) 621-625.
[29] A. Phukan, J.N. Ganguli, D.K. Dutta, $ZnCl_2$-Zn^{2+}-Montmorillonite composite: efficient solid acid catalyst for benzylation of benzene, J. Mol. Catal. A: Chem. 202 (2003) 279-287.